International Journal of Medical Laboratory 2016;3(4):270-281.

International Journal of Medical Laboratory
Shahid Sadoughi University of Medical Sciences

Original Article

A Stereological Study on Hippocampal Subfields Following Administration of Methamphetamine in Male Mice

Sanaz Hadizade Asar M.Sc., Mohammad Hosseini-Sharifabad* Ph.D., Maryam Yadegari Ph.D.

Department of Anatomical Sciences, Faculty of Medicine, Shahid Sadoughi University of Medical Science Yazd, Iran.

Article history
Received 2 Oct 2016
Accepted 27 Nov 2016
Available online 28 Jan 2017

Key words
Hippocampus
Methamphetamine
Mice
Stereology

A B S T R A C T

Background and Aims: This study examined sub-chronic effects of Methamphetamine (METH) on the stereological parameters in the Cornu Ammonis (CA) of the hippocampus in adult mice.

Materials and Methods: Fifteen adult male mice, eight weeks old, were randomly divided into three groups: receive saline (controls), or low-dose (LD) 2.5 mg/kg METH, or high-dose (HD) 25 mg/kg METH, via daily intraperitoneal administrations for one month. The Cavalieri principle was used to estimate the volume of CA hippocampal field. The physical disector was used to determine the numerical density of CA1 and CA3 pyramidal cells. The qualitative Golgi staining was also done for analyzing the dendritic morphology of CA1 and CA3 pyramidal cells.

Results: Our results showed that in METH-treated mice, the volumes of the Oreins, Pyramidal and Radiatum-Lacunosum-Moleculare layers in the CA1 and CA3, the entire volumes of the CA1 and CA3 subfields and the entire hippocampal volume were significantly increased compared to the control animals ($p<0.001$). The estimated total number and numerical density of pyramidal cells in the CA1 and CA3 in both treated groups showed a significant decrease in comparison with the controls ($p<0.001$). The pyramidal neurons of CA1 and CA3 in treated mice had more dendritic arborization and greater dendritic length than control mice.

Conclusions: Our findings indicate that sub-chronic METH injection induces stereological changes in the structure of the hippocampus in adult mice. A neuroanatomical basis may be related to the primarily reported impairment of learning and memory abilities in the METH user.

*Corresponding Author: Department of Anatomical Sciences, Faculty of Medicine, Shahid Sadoughi University of Medical Science Yazd, Iran. **Tel:** +98 9133536199; **Fax:** +98 351 6238561; **Email:** mhosseini81@yahoo.com

Introduction

Abuse of the illicit psychotropic, methamphetamine (METH) has become a serious social and public concern [1]. The detriments of regular use of METH consist severe neurologic and psychiatric disturbance including hallucinations, delusions, as well as anxiety and depression [2]. Many reports reveal numerous neuropathological disorders such as Parkinson's disease, Alzheimer's disease, Schizophrenia and Bipolar disorder in METH-exposed individuals [3, 4]. METH damages dopaminergic and serotonergic neuronal terminals, resulting in decreased of dopamine-serotonin uptake, leading to an increase in synaptic space monoaminergic neurotransmitter levels by its pharmacological effects [5]. Previous studies have represented that increased glutamate release, mitochondrial damage, neuroinflammation, hyperthermia and oxidative stress contributes to METH-induced neurotoxicity [6, 7]. Additionally, administration of METH causes many destructive effects on the various organs in the body, including the kidneys, respiratory system, heart and liver [8-10]. However, numerous studies of METH have focused on the limbic region of the brain, especially the hippocampus [11, 12]. Laboratory animals studies have shown that the hippocampus, a critical region in the middle of temporal lobes in the brain, is a very delicate area that appears to be significantly vulnerable to METH toxicity effects during the developmental period [13, 14]. Recent reports in human and non-human primates using magnetic resonance imaging extensively have demonstrated structural abnormalities in the hippocampus of METH users, such as enhanced white-matter volumes, lower gray-matter volumes, and higher white-matter hyperintensities [15, 16]. Moreover, the previous research has suggested that long-term injection of METH can cause a reduction in the size of cereblum and reduced number of cerebellar neurons. [17]. It has also been reported decrease in the hippocampal neurogenesis in METH exposure. It can be associated with maladaptive hippocampal plasticity, which due to cognitive impairments like deficits in memory and learning [18, 19]. In spite of several types of researchs examining the adverse effects of METH on structure and function of the hippocampus qualitatively, there are a few studies that quantitatively examine its effects on the structure of this brain's region. So, this study aimed to provide unbiased estimates of the total number of pyramidal neurons, the volume of CA1 and CA3 subfields and morphology of pyramidal neurons of the hippocampus influenced by subchronic METH exposure in mice by stereological and histological methods.

Materials and methods

Animal and treatment

In this experimental study, eight weeks old adult male Balb/c mice (from animal house of Shahid Sadoughi medical faculty, Yazd, Iran) weighing 45 grams on average were used. The mice were housed in cages at temperature-

controlled (22±2ºC) animal room, with 12 hours alternating light / dark cycle (light on at 07.00-19.00 hours) and allowed free access to food and water ad libitum. Group I and II (experimental groups), received low-dose METH (2.5 mg/kg) [20] and high-dose METH (25 mg/kg) [21]. Bothwere administered in a volume of 1 ml/kg body weight, via daily intraperitoneal (I.P) injections for 30 days; group III, comprised of healthy normal mice received I.P saline in a similar volume given to the experimental animals. Experimental procedures were carried out according to Shahid Sadoughi university of medical sciences, Ethical Committee acts.

Histological procedures

The animals were fully anesthetized using ketamine (Merck, Germany), perfused transcardiacally with a phosphate-buffered solution of 4% formaldehyde and 1% glutaraldehyde for fixation. Following perfusion, the brains were taken out carefully from the skull by craniotomy. Each brain was separated from the midsagittal line and divided into hemispheres. One hemisphere was selected at random for estimating the volumes of the CA1 and CA3 sublayers and the numerical density of pyramidal neurons in both subfields, and the other was used for morphological analysis of CA1 and CA3 pyramidal neuron dendrites. The tissue samples were passed through a series of ascending alcohol solutions for dehydration, cleared with xylene and then were placed in paraffin for sectioning. The serial coronal sections (5 µm) were sliced from the full thickness of the hippocampus using a rotatory microtome (Zeiss Microm International GMBH, Walldorf, Germany). A total of 1400-1600 sections were sliced along the whole paraffin block embedding brain tissue. From the tissue sections cut, ten pairs sections were systematic and uniformly sampled with a random start in the first 150 sections. The sections were mounted directly onto glass slides and dried in air at room temperature for staining. The slide-mounted sampled sections were stained with toluidine blue (Merck, Germany) for estimating the number of neurons and routine hematoxylin and eosin (Sigma, USA) for the volume. As well as, the numbers of thick sections with a thickness of 100µm were cut from another cerebral hemisphere to evaluate the morphological characteristics of CA1 and CA3 pyramidal neurons dendrites. The slide-mounted tissue sections were stained with silver nitrate solution (Merck, Germany).

Hematoxylin and Eosin staining

The slide-mounted sampled sections deparaffinized in xylene before staining, rehydrated in 100%, 70% ethanol for 5 min and in distilled water 5 min. Next the sections were stained in hematoxylin solution for 5 min and then rised quickly in running water. After decolorization in 75% ethyl alcohol for few seconds, the sections were stained in eosin Y solution for 2 min. the sections were then dehydrated in 95% , 100% ethanol for 5 min and mounted in Enthellan (Merck, Darmstadt, Germany) [22].

Toluidine blue staining

The slide-mounted sampled sections were stained in 0.03% toluidine blue solution (PH=1.5) for 1–2 min. after dry in air, rinsed with dH2O, then decolorized in 75% ethyl alcohol and dehydrated in 95%, 100% ethyl alcohol for 2 to 3 min. The sections were then

cleared in xylene for 2 to 3 min. and cover glasses were mounted [23].

Golgi staining

The slides of hippocampal samples were stained with silver nitrate solution according to the Hu et al. [24]. At first, a block of formaldehyde hippocampal tissue was immersed into 2% aqueous solution of potassium dichromate for two days. Then, the blocks were dried with a filter paper. The specimens were then transferred into 2% aqueous solution silver nitrate and stored in the dark for two days. The tissue was sectioned 100 µm thick. The tissue slices were dehydrated quickly cleared and mounted on gelatin-coated slides and coverslipped [25].

Estimation of tissue volume

To volumetric analysis of CA1 and CA3 sublayers, the photography was performed under the 10x objective lens (Olympus, Japan), and total magnification was 110x. The Cavalieri's Principle [26] is a method for determining the reference volumes of the hippocampal CA1 and CA3 sublayers by using the point-counting grid. A transparent grid was randomly placed over the sublayers of each sampled section. Points that hit each layer of CA1 and CA3 were counted. The reference volume was calculated by the following formula:

$$V_{ref} = \sum pi \times A(pi) \times t$$

Wh ere $\sum pi$ is the total number of grid points appeared in sections, $A(pi)$ is the area associated with each grid point and t is the known distance between sections.

Estimation of cell density

The pyramidal cell density in pyramidal cell layer of CA1 and CA3 was determined via the physical disector method [27] with the following formula:

$$Nv = \sum Q/N\ (dis) \times V\ (dis)$$

Where $\sum Q$ is the total number of pyramidal cells counted (nucleolus as counting units) in each disector frame of sampled sections, $N(dis)$ is the sum of all counted disector frames, $V(dis)$ is the volume of disector frame:

$$V(dis) = A(frame) \times h$$

Where $A(frame)$ is the known area associated with each disector frame and h is the height of section and was equal to the section thickness. For the estimation of the density of hippocampal CA1 and CA3 pyramidal cells, two serial sections were observed with 100x objective lens and total magnification was 1100x. If the nucleolus of a cell was located entirely inside the counting frame or contact with the inclusion lines of the one section (reference section) were counted, whereas those in touch with the exclusion lines of the adjacent serial section (look-up section) were excluded. The total number of pyramidal cells were estimated by multiplying the measures of the reference volume *"V(ref)"* of the sublayers by the measures of the numerical density, *"Nv"*.

Statistical analysis

Data were expressed as mean±standard deviation (SD). Statistical comparisons were performed using one-way ANOVA followed by Bonferroni post hoc test. All statistical analysis was carried out using SPSS software, version 19. Differences were defined as $p<0.05$.

Results

Comparison of the three groups showed reductions in the both total number (Fig. 1) and the numerical density of pyramidal CA1 and CA3 of hippocampus in experimental groups compared with controls (Fig. 2, Fig. 3). While statistically, a significant cell reduction was only seen in CA1 region of METH groups ($p<0.05$). Data showed METH-treated mice significantly had larger volumes than controls in total volume of CA1 and CA3 subfields and in its Oriens, Pyramidal, and Radiatum-Lacunosum-Moleculare layers in low-dose and high-dose groups. Although, the increase in the CA1 and CA3 Radiatum-Lacunosum-Molecular layer was statistically significant only in high-dose groups ($p<0.05$) (Fig. , Fig. , and Fig.). This study also revealed that the entirevolume of Cornu Ammonis was significantly greater in METH-treated mice than their controls ($p<0.05$). The results of qualitative analysis also showed that in these neurons, the dendritic arborization, and dendritic length was greater in the METH-treated in compared with the control mice. While, the increase in dendritic length and arborization in the CA3 region was not observed (Fig.).

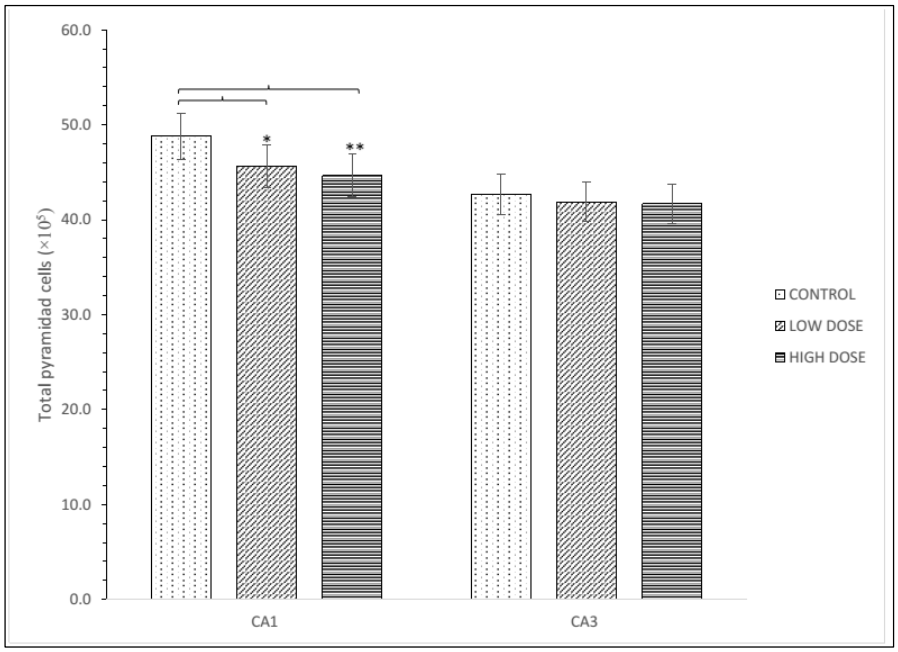

Fig. 1. Bar graphs showing the total number of CA1 and CA3 pyramidal neurons of hippocampus in METH-treated mice and control. Each bar represents the mean±SEM. * $p<0.05$, ** $p<0.001$.

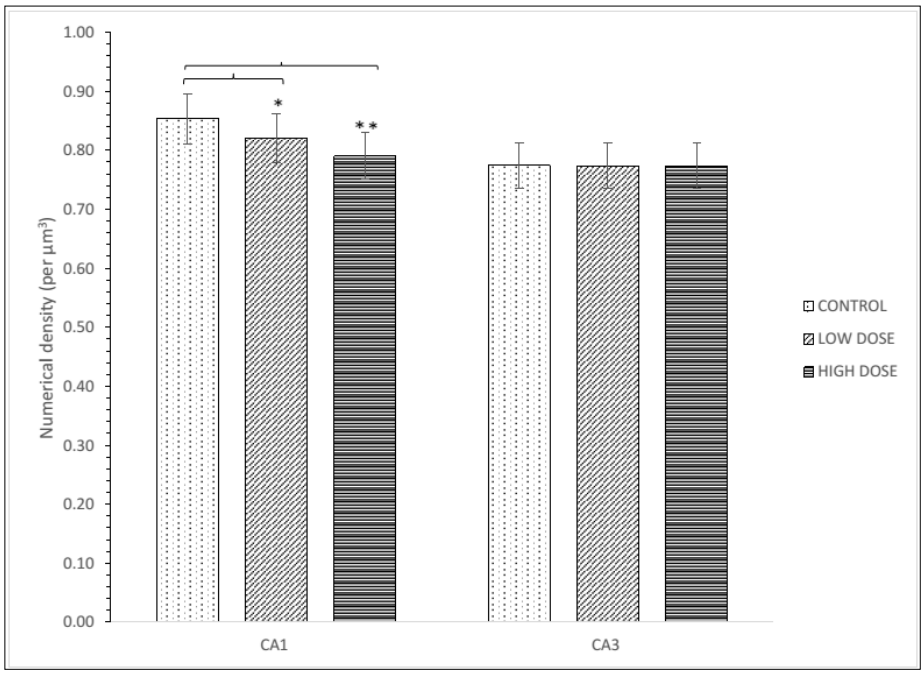

Fig. 2. Bar graphs showing the numerical density of CA1 and CA3 hippocampal of pyramidal neurons of METH-treated mice and control. Each bar represents the mean ± SEM. * $p<0.05$, ** $p<0.001$.

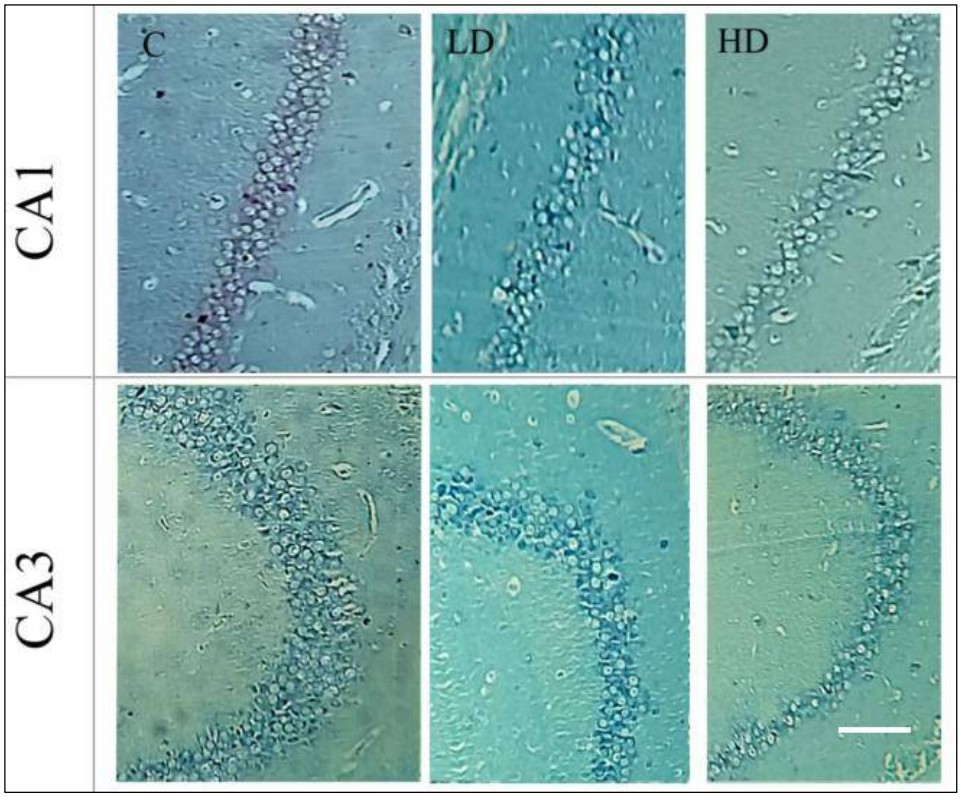

Fig. 3. Representative photomicrographs of a coronal section of the Cornu Ammonis (CA) of the hippocampus of adult mice stained with toluidine blue. Note a decrease in the numerical density of pyramidal neurons in methamphetamine (METH)-treated mice compared with controls. Scale bars=50 µm, C= control, LD= low dose, HD= high dose.

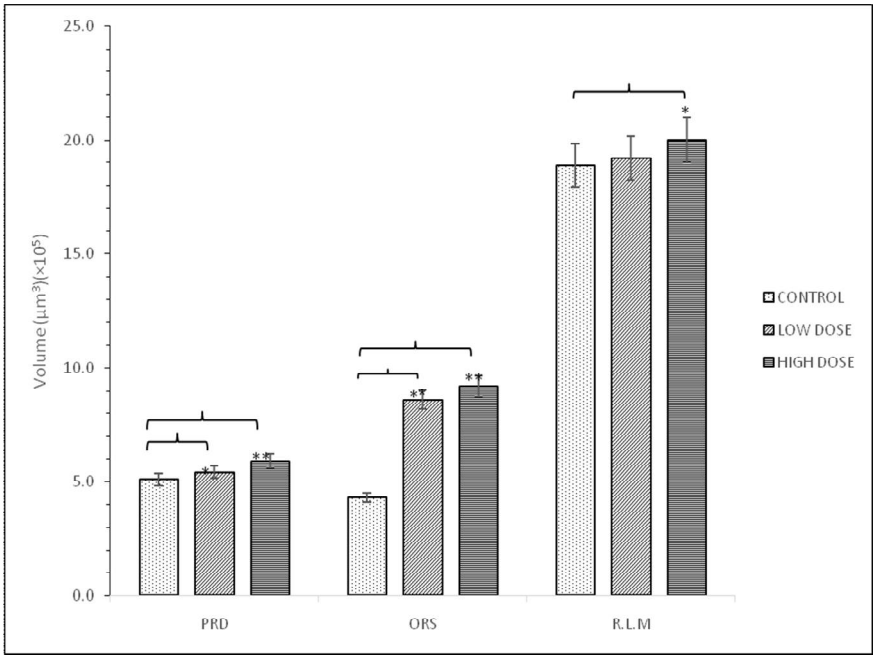

Fig. 4. Bar graphs showing the volume of CA1 Pyramidal (PRD), Oriens (ORS), and Radiatum-Lacunosum-Moleculare(R.LM) layers of METH-treated mice and control. Each bar represents the mean ± SEM. * $p<0.05$, **$p<0.001$.

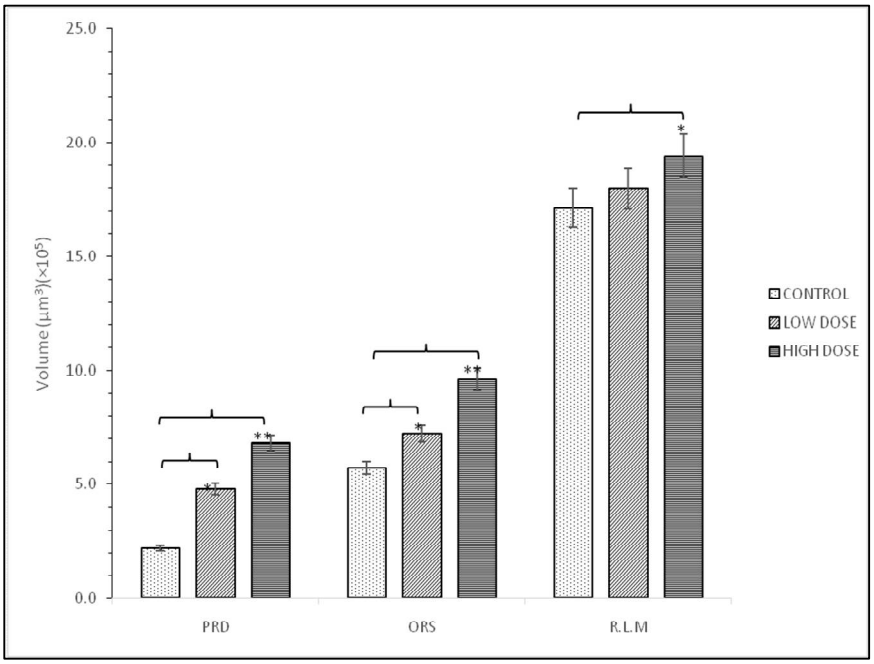

Fig. 5. Bar grafs showing the volume of CA3 Pyramidal (PRD),Oriens (ORS), and Radiatum-Lacunosum-Moleculare (R.LM) layers of METH-treated mice and control. Each bar represents the mean ± SEM. * $p<0.05$, $p<0.001$.

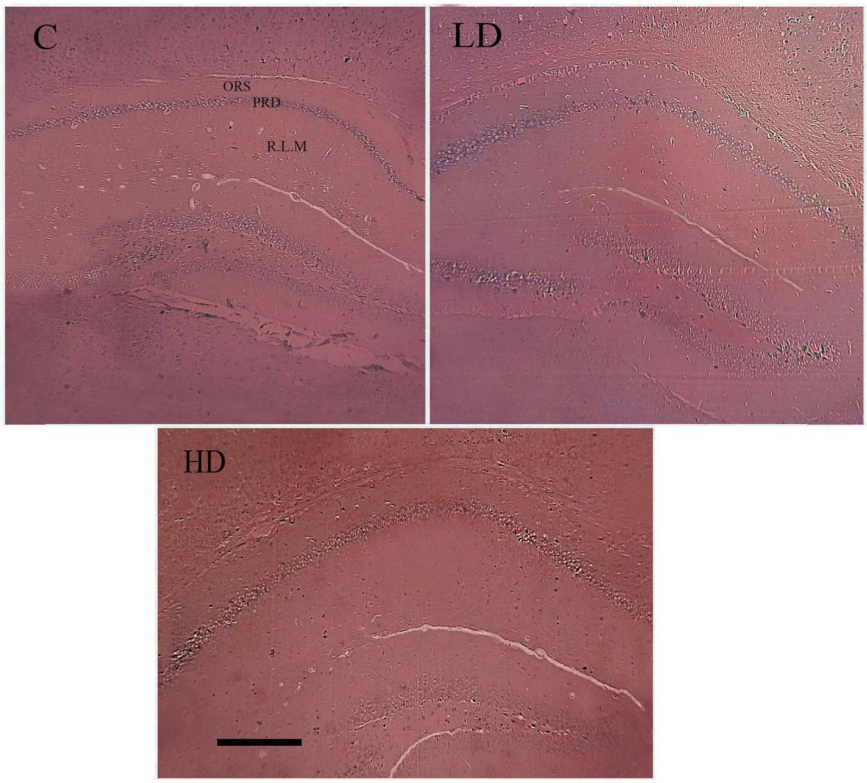

Fig. 6. Representative photomicrographs of a hematoxylin-eosin stained coronal sections through the Cornu Ammonis (CA) of the hippocampus of adult mice showing significant increased volume in healthy control mice (C), low-dose methamphetamine (METH)-administrated mice (LD) and high-dose METH-administrated mice (HD). ORS; Oriens, PRD; Pyramidal, RLM; Radiatum-Lacunosum-Molecular. Scale bars=200 µm, C= control, LD= low dose, HD= high dose.

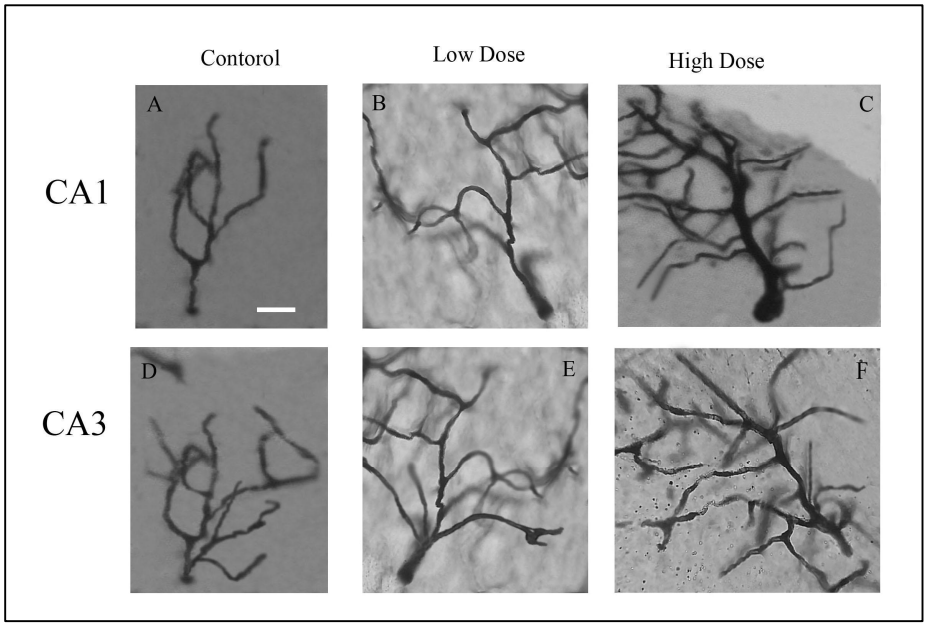

Fig. 7. Photomontages of Golgi-impregnated CA1(A-C) and CA3 (D-F) pyramidal cells. Neurons from control mice are shown in the left column (A, D), from low-dose methamphetamine (METH)-treated mice in the inner column (B, H) and high-dose METH-treated mice (C, F) in the right column. Observe the increase in dendritic length and arborization in METH-treated mice compared to controls. Scale bars=50 µm (applies to A-F frames).

Discussion

The main findings of this study by using the design-based stereological methods were: Subchronic administration of METH-induced significant volumetric change in the sublayers of the hippocampal CA1 and CA3 in adult male mice. Subchronic exposure to METH leads to alterations in numerical density and a total number of hippocampal CA1 and CA3 pyramidal neurons. Subchronic METH exposure induced changes in Golgi-stained hippocampal CA1 and CA3 pyramidal neurons dendrites. This study is the first research, to our knowledge, examining the deleterious effects of hallucinogenic methamphetamine on the stereological characteristics of hippocampal CA1 and CA3 subfields together with a morphological analysis of pyramidal neurons in the hippocampus. The quantitative findings of the current study revealed a significant decrease in numerical density and a total number of pyramidal cells in the hippocampal CA1 and CA3 subregions in both METH-treated groups compared to the control group. However, the reductions in the CA3 pyramidal cell layer did not reach statistically significant level, perhaps because of the pharmacological and neurotoxicological properties of methamphetamine. Additionally, previous studies have shown that pyramidal cells of the CA1 hippocampal subfield are more sensitive to cytotoxic effects of METH exposure than are those of the CA3 subfield of the hippocampus [28, 29]. An earlier behavioral and structural experiment demonstrated that prenatal carbamazepine treatment leads to a reduction of hippocampal CA1 and CA3 and cortical neurons without scrutable effects on cognitive functions [30]. Reports by Gokcimen et al. suggested that the single dose of anti-inflammatory administration decreases the total number of CA1 and CA3 pyramidal neurons and dentate granule cells [31]. To date, there are a few published reports about the mechanisms of reduction in cell populations following METH administration. Newly, several lines of evidence have indicated that METH can cause neuropathological variation within multiple brain areas by inducing apoptotic pathways [32]. For example, using TUNNEL histochemical approach, neuronal apoptosis in the mouse brains have been observed following single administration of METH (40mg/kg) [33]. Similarly, another previous study pointed that mitochondrial damage, endoplasmic reticulum stress and activation of caspase-3 leading to induction of apoptosis caused by METH [34]. In addition to apoptotic cell death, the number of studies in the literature has documented that morphologically necrotic neurons following METH treatment [35, 36]. Moreover, recently in vivo and in-vitro METH-exposed animal studies also illustrated a decrease in hippocampal progenitor cells proliferations in a dose-dependent manner [37, 38]. This effect correlated with the fragmentation of mitochondrial network architecture [39]. It was also noted in our study an increased hippocampal entire volume with increase in the entire volume of hippocampal CA1 and CA3 and its sublayers in both experimental groups

compared to the control group. However, an increase in the entire volume of the CA1 subfield and its Radiatum-Lacunosum-Molecularesublayer was not significant in the low-dose groups compared to the controls. It could be due to inflammatory changes in this brain region [40]. Sarsilmaz et al. suggested that exposing neonatal rats to a high-dose of formaldehyde at PND90 increased the volume of the pyramidal layer of CA, whereas this increase observed in low-dose of formaldehyde at PND30 in a dose- and age- dependent manner [41]. In another animal study, it was found that exposed to nicotine during the brain growth spurt have been published to show a significant increase in the volume of the cerebellar vermis [42]. Qualitative morphological analysis of Golgi-stained CA1 and CA3 hippocampal neurons revealed greater dendritic length and arborization in METH-treated groups compared with controls. So, we speculated a compensatory reaction in response to the reduction of the pyramidal cells in both regions. Inconsistent with our results, it was described by Kamali et al. that METH-administrated mice showed a notable decrease in the number of Purkinje cells and granular cells of the cerebellum. However, they found a reduction in the volume of the cerebellar-sublayers, which is in contrast to our findings [17]. It has also been demonstrated that multiple doses of amphetamine had no alterations in the pyramidal cells number and the volume of hippocampal CA1 and CA3 fields [43]. This disparity may be related the dose of METH exposure, treatment duration and method of estimating stereological parameters.

Conclusion

We have indicated that exposure to METH has significant effects on the volume of CA1 and CA3 subfields and the pyramidal cell numbers in the hippocampus. The mechanisms responsible for METH-induced hippocampal injury remain unclear at present. Further studies are required to illuminate the diverse mechanisms by which METH created these effects in the developing CNS to develop conceivable prevention or treatment strategies versus toxicity of methamphetamine.

Conflict of Interest

The authors declare that they have no conflict of interest.

Acknowledgments

There is no acknowledgment to declare.

References

[1]. Xue X, Yang JY, He Y, Wang LR, Liu P, Yu LS, et al. Aggregated single-walled carbon nanotubes attenuate the behavioural and neurochemical effects of methamphetamine in mice. Nat Nanotechnol. 2016; 11(7): 613-20.

[2]. Ahmadi J. Fast Treatment of Methamphetamine Related Anxiety and Depressive Disorders: A Novel Approach. J Addict Med Ther Sci. 2016; 2(1): 001-003.

[3]. Fassbender C, Lesh TA, Ursu S, Salo R. Reaction Time Variability and Related Brain Activity in Methamphetamine Psychosis. Bio Psychiatry 2015; 77(5): 465-74.

[4]. Yu S, Zhu L, Shen Q, Bai X, Di X. Recent Advances in Methamphetamine Neurotoxicity Mechanisms and Its Molecular Pathophysiology. Behav Neurol. 2015; 2015(2): 60-71.
[5]. Halpin LE, Collins SA, Yamamoto BK. Neurotoxicity of methamphetamine and 3, 4-methylenedioxymethamphetamine. Life Sci. 2014; 97(1): 37-44.
[6]. Baptista S. Impact of methamphetamine on dentate gyrus neurogenesis: the underlying mechanisms and the role of neuropeptide Y. [PhD Thesis]; 2015.
[7]. Huang Y-N, Yang L-Y, Wang J-Y, Lai C-C, Chiu C-T, Wang J-Y. L-Ascorbate Protects Against Methamphetamine-Induced Neurotoxicity of Cortical Cells via Inhibiting Oxidative Stress, Autophagy, and Apoptosis. Mol Neurobiol. 2017; 54(1): 125-36.
[8]. Hassan SF, Wearne TA, Cornish JL, Goodchild AK. Effects of acute and chronic systemic methamphetamine on respiratory, cardiovascular and metabolic function, and cardiorespiratory reflexes. J Physiol. 2016; 594(3): 763-80.
[9]. Kaye S, Darke S, Duflou J, McKetin R. Methamphetamine-related fatalities in Australia: demographics, circumstances, toxicology and major organ pathology. Addict. 2008; 103(8): 1353-60.
[10]. Lineberry TW, Bostwick JM. Methamphetamine abuse: a perfect storm of complications. Mayo Clinic Proceed. 2006; 81(1): 77-84.
[11]. Zhu R, Yang T, Kobeissy F, Mouhieddine TH, Raad M, Nokkari A, et al. The Effect of Chronic Methamphetamine Exposure on the Hippocampal and Olfactory Bulb Neuroproteomes of Rats. PloS one 2016; 11(4): e0151034.
[12]. Thompson PM, Hayashi KM, Simon SL, Geaga JA, Hong MS, Sui Y, et al. Structural abnormalities in the brains of human subjects who use methamphetamine. J Neurosci. 2004; 24(26): 6028-36.
[13]. Kiernan J. Anatomy of the temporal lobe. Epilepsy research and treatment. 2012; 2012: 176157
[14]. Park M, Kim H-J, Lim B, Wylegala A, Toborek M. Methamphetamine-induced occludin endocytosis is mediated by the Arp2/3 complex-regulated actin rearrangement. J Biol Chem. 2013; 288(46): 33324-3334.
[15]. Morales A, Kohno M, Robertson C, Dean A, Mandelkern M, London E. Gray-matter volume, midbrain dopamine D2/D3 receptors and drug craving in methamphetamine users. Mol Psychiatry 2015; 20(6): 764-71.
[16]. Berman S, O'Neill J, Fears S, Bartzokis G, London ED. Abuse of amphetamines and structural abnormalities in the brain. Ann N Y Academy Sci. 2008; 1141(1): 195-220.
[17]. Kamali Ardakani R, Nahangi H, Yadegari M, Hosseini-Sharifabad M. The Effects of Long-Term Administration of Methamphetamine on the Cerebellum of the Male Mice: a Stereological Study. The Neuroscience Journal of Shefaye Khatam. 2014; 2(4): 37-45.
[18]. Galinato MH, Orio L, Mandyam CD. Methamphetamine differentially affects BDNF and cell death factors in anatomically defined regions of the hippocampus. Neurosci. 2015; 286: 97-108.
[19]. Ekthuwapranee K, Sotthibundhu A, Govitrapong P. Melatonin attenuates methamphetamine-induced inhibition of proliferation of adult rat hippocampal progenitor cells in vitro. J Pineal Res. 2015; 58(4): 418-28.
[20]. Chiu C-T, Ma T, Ho K. Attenuation of methamphetamine-induced behavioral sensitization in mice by systemic administration of naltrexone. Brain Res Bull. 2005; 67(1): 100-109.
[21]. Yamanaka Y, Takano R, Egashira T. Methamphetamine induced behavioral alterations following repeated administration of methamphetamine. Jpn J Pharmacol. 1986 Jun;41(2):147-54
[22]. Sakamoto K, Matsushita Y, Minamizato T, Katsuki Y, Katsube K-i, Yamaguchi A. The Bone Regeneration Model and Primary Osteoblastic Cell Culture Used in the Analysis of Ccn3 Transgenic and Knockout Mice. Methods Mol Biol. 2017; 1489: 309-24.
[23]. Zhu Y, Liu F, Zou X, Torbey M. Comparison of unbiased estimation of neuronal number in the rat hippocampus with different staining methods. J Neurosci Methods 2015; 254: 73-9.
[24]. Hu F, Ge MM, Chen WH. Effects of lead exposure on dendrite and spine development in hippocampal dentate gyrus areas of rats. Synapse 2016; 70(3): 87-97.
[25]. Zaqout S, Kaindl AM. Golgi-Cox staining step by step. Front Neuroanat. 2016; 10: 38.
[26]. Gundersen H, Bendtsen TF, Korbo L, Marcussen N, Møller A, Nielsen K, et al. Some new, simple and efficient stereological methods and their use in pathological research and diagnosis. Apmis. 1988; 96(1-6): 379-94.
[27]. Miki T, Satriotomo I, Li HP, Matsumoto Y, Gu H, Yokoyama T, et al. Application of the physical disector to the central nervous system: estimation of the total number of neurons in subdivisions of the rat hippocampus. Anatomic Sci Int. 2005; 80(3): 153-62.
[28]. Ijomone O, Nwoha P, Olaibi O, Obi A, Alese M. Neuroprotective effects of kolaviron, a biflavonoid complex of Garcinia kola, on rats hippocampus against methamphetamine-induced neurotoxicity. Macedonian J Med Sci. 2012; 5(1): 10-6.
[29]. Sen R, Shaffi S, Kakaria V, Chauhan A. Histological Studies of the Effects Of

Dichloroacetic Acid (DCA) Exposure on The Hippocampus of Male Albino Rats. Bull Env Pharmacol Life Sci. 2015; 5(1): 28-32.
[30]. Åberg E, Holst S, Neagu A, Ögren SO, Lavebratt C. Prenatal exposure to carbamazepine reduces hippocampal and cortical neuronal cell population in new-born and young mice without detectable effects on learning and memory. PloS one 2013; 8(11): e80497.
[31]. Gokcimen A, Rağbetli MÇ, Baş O, Tunc AT, Aslan H, Yazici AC, et al. Effect of prenatal exposure to an anti-inflammatory drug on neuron number in cornu ammonis and dentate gyrus of the rat hippocampus: a stereological study. Brain Res. 2007; 1127(1): 185-92.
[32]. Cadet JL, Jayanthi S, Deng X. Speed kills: cellular and molecular bases of methamphetamine-induced nerve terminal degeneration and neuronal apoptosis. FASEB J. 2003; 17(13): 1775-88.
[33]. Deng X, Wang Y, Chou J, Cadet JL. Methamphetamine causes widespread apoptosis in the mouse brain: evidence from using an improved TUNEL histochemical method. Mol Brain Res. 2001; 93(1): 64-9.
[34]. Courtney KE, Ray LA. Methamphetamine: an update on epidemiology, pharmacology, clinical phenomenology, and treatment literature. Drug Alcohol Depend. 2014; 143: 11-21.
[35]. Tulloch I, Afanador L, Mexhitaj I, Ghazaryan N, GarzaGongora AG, Angulo JA. A single high dose of methamphetamine induces apoptotic and necrotic striatal cell loss lasting up to 3 months in mice. Neurosci. 2011; 193: 162-69.
[36]. Fujikawa DG, Pais ES, Aviles ER, Hsieh K-C, Bashir MT. Methamphetamine-induced neuronal necrosis: the role of electrographic seizure discharges. Neurotoxicol. 2016; 52: 84-8.
[37]. Baptista S, Lasgi C, Benstaali C, Milhazes N, Borges F, Fontes-Ribeiro C, et al. Methamphetamine decreases dentate gyrus stem cell self-renewal and shifts the differentiation towards neuronal fate. Stem Cell Res. 2014; 13(2): 329-41.
[38]. Venkatesan A, Uzasci L, Chen Z, Rajbhandari L, Anderson C, Lee M-H, et al. Impairment of adult hippocampal neural progenitor proliferation by methamphetamine: role for nitrotyrosination. Mol Brain 2011; 4(1): 1-14.
[39]. Tian C, Murrin LC, Zheng JC. Mitochondrial fragmentation is involved in methamphetamine-induced cell death in rat hippocampal neural progenitor cells. PloS one 2009; 4(5): e5546.
[40]. Thanos PK, Kim R, Delis F, Ananth M, Chachati G, Rocco MJ, et al. Chronic Methamphetamine Effects on Brain Structure and Function in Rats. PloS one 2016; 11(6): e0155457.
[41]. Sarsilmaz M, Kaplan S, Songur A, Colakoglu S, Aslan H, Tunc AT, et al. Effects of postnatal formaldehyde exposure on pyramidal cell number, volume of cell layer in hippocampus and hemisphere in the rat: a stereological study. Brain Res. 2007; 1145: 157-67.
[42]. Chen W-JA, King KA, Lee RE, Sedtal CS, Smith AM. Effects of nicotine exposure during prenatal or perinatal period on cell numbers in adult rat hippocampus and cerebellum: a stereology study. Life Sci. 2006; 79(23): 2221-227.
[43]. Smith AM, Pappalardo D, Chen W-JA. Estimation of neuronal numbers in rat hippocampus following neonatal amphetamine exposure: a stereology study. Neurotoxicol Teratol. 2008; 30(6): 495-502.